Some effects of the doping α-Al_2O_3 nanoparticles in the transport properties of $Bi_{1.65}Pb_{0.35}Sr_2Ca_2Cu_3O_y$ ceramic superconductors

M. Hernández-Wolpez
Departamento de Física Universidad de Camagüey,
Ctra. Circunvalación Norte, Km 5 1/2, Camagüey, Cuba,
e-mail: manuel.hwolpes@reduc.edu.cu

I. García-Fornaris
Departamento de Ciencias Básicas Universidad de Granma,
Apartado 21, Box 85100, Bayamo, Cuba,

E. Govea-Alcaide
Departamento de Física, Universidade Federal do Amazonas,
Av. General Rodrigo Octávio, 6200 Coroado I, 69077-000 Manaus, Brazil.

R.F. Jardim
Instituto de Física, Universidade de São Paulo,
66318, 05314-970, São Paulo, SP, Brasil

P. Muné
Departamento de Física, Universidad de Oriente,
Patricio Lummumba s/n, P. O. Box 90500, Santiago de Cuba, Cuba

Received 9 June 2017; accepted 13 December 2017

We present a preliminary study on the effects of nano-size α-Al_2O_3 (40 nm) in the transport properties of $Bi_{1.65}Pb_{0.35}Sr_2Ca_2Cu_3O_y$ ((Bi,Pb)-2223) ceramic samples. The (Bi,Pb)-2223 samples were synthesized by the solid state reaction method and α-Al_2O_3 nanoparticles (NPs), with concentrations ranging from 0.1 to 0.7 wt. percent (% wt.), were added before the last heat treatment. All samples were characterized by means of X-rays diffraction patterns, and temperature and magnetic field dependence of the electrical resistivity, $\rho(T, B_a)$. From the experimental $\rho(T, B_a)$ data we extracted the critical temperature dependence of the % wt. of α-Al_2O_3 NPs, and by using the Arrhenius plot the effective pinning energy has been also determined. The results indicate that mostly of the transport properties are optimized for the sample doped with 0.3% wt. of α-Al_2O_3 NPs.

Keywords: (Bi; Pb)-2223; transport properties; doping; effects of the material synthesis.

PACS: 74.72.Hs; 74.25.Fy; 74.62.Dh; 74.62.Bf

1. Introduction

Among the high-Tc (HTc) superconductors, the (Bi,Pb)-2223 is the best candidate for the applications at liquid-nitrogen temperature [1], due to the critical parameters values: critical temperature of the superconducting transition ($T_c \sim 108$ K), critical current density ($J_c \sim 10^6$ A/cm^2), second critical field ($H_{c2} > 100$ T) and the full penetration field ($H^* \sim 0.2$ T) both measured to 4 K; and also for the fundamental lengths: coherence length ($\xi = 1.5$ nm) and the penetration depth of the magnetic field ($\lambda = 150$ nm) [2]. Moreover, the pinning potential is one of the basic parameters that defines the performance of a superconducting material for commercial and technological applications [3]. In general, the granular superconducting materials can be modified into a material with better transport properties, for example: varying the compacting pressure [4, 5], varying the sintering time [6], by chemical doping and nanosized particles addition [7–10]. For example, Ghattas *et al*. [3] analyzed the effects of α-Al_2O_3 NPs addition on the microstructure and pinning properties of polycrystalline (Bi,Pb)-2223 samples. From the analysis of X-rays diffraction patterns, the authors obtained that addition of α-Al_2O_3 NPs up to 0.3% wt. does not affect (Bi, Pb)-2223 phase formation, which was estimated in order to $\sim$ 90%. The addition of 0.2% wt. of α-Al_2O_3 NPs increased the critical current density and improved the J_c behavior in applied magnetic field. They analyzed the pinning force, and the results imply that the enhancement of the vortex flux pinning in 0.2% wt. of α-Al_2O_3 doped sample mainly originated from the surface normal-like pinning center. In this paper, from the experimental data of the resistivity as a function of temperature and applied magnetic field, $\rho(T, Ba)$, the critical temperature as function of % wt. of the α-Al_2O_3 NPs dependence was obtained and using the Arrhenius plot the effective pinning energy was determined. The results reveals that, in general, the transport properties were optimized for the sample doped with 0.3% wt. of α-Al_2O_3 NPs. It is well known that nanoparticles act as artificial pinning centers inside the superconducting materials. For that reason, this preliminary study allows us select

TABLE I. Comparison between the methods of obtaining of the samples used by Ghattas *et al.* [3] and in this paper.

Differences	Ghattas *et al*. [3]	In this paper
Powders added	5% of PbO and (0.1-0.8)% of α-Al_2O_3 NPs	(0.1-0.7)% of α-Al_2O_3 NPs
Compacting pressure	1 GPa	249 MPa
Sintering temperature	830°C	845°C
Sintering time	72 h	12 h

a sample set more reduced to analyze later more details studies related with the doping effects with α-Al_2O_3 NPs on the penetration and trapping mechanisms of the magnetic flux in (Bi,Pb)-2223 superconducting ceramics to extend recent studies of our research group [11–13] done in other type of Bi-based ceramic superconductor. For that reason, the Ghattas and co-authors work [3] was the most important paper for support and compare our results.

2. Experimental

Polycrystalline samples of $Bi_{1.65}Pb_{0.35}Sr_2Ca_2Cu_3O_y$ ((Bi,Pb)-2223) were prepared from powders: Bi_2O_3, PbO, $SrCO_3$, $CaCO_3$ and CuO, were mixed in an atomic ratio of Pb:Bi:Sr:Ca:Cu (0.35:1.65:2:2:3). The mixture was first calcined in air at 750 °C for 40 h. Then, the poder was reground and pressed into pellets of 10 mm in diameter and 2 mm in thickness at a pressure of 196 MPa. These pellets were heat treated at 800°C in air for 40 h. Subsequently, the samples were reground, pressed again, and sintered in air at 845°C in air for 40 h. This step was repeated three times, as described elsewhere [14, 15]. The α-Al_2O_3 NPs with concentrations ranging from 0.0 to 0.7% wt. (correspond with B00 to B07 samples code) were added before the last heat treatment in presence of isopropanol to avoid the nanoparticles agglomerations. The alcohol was evapoted while the mixture has been shaken. Finally the powder were reground and pressed uniaxially at 249 MPa to obtain cylindrical samples with dimension of $d = 10$ mm in diameter and 2 mm in thickness. The last treatment of the pellet was performed in air at 845°C for 12 h followed by slow cooling.

In the Table I the obtaining methods followed by Ghattas and co-workers [3] with the followed in this paper were compared. The little differences between the Ghattas and our results, could be due to the method used in both works. For example, the influence of compacting pressure modified the transport properties [4, 5]; the sintering time variation [6] can modified these properties too. Beyond of the different method used in these papers, the main results are very similar.

The X-rays diffraction patterns were obtained by means of Bruker-AXS D8 Advance diffractometer. These diffraction patterns were compared regarding a diffractogram of another sample as a pattern to evaluate the influence of the doping with α-Al_2O_3 NPs in the material structure. These measurements were performed at room temperature using CuKα radiation in the $3° \leq 2\theta \leq 80°$ range with a step 0.02° in 2θ size and 5 s counting time with θ-2θ geometry.

The temperature dependence of the electrical resistivity for different values of applied magnetic field, $\rho(T, B_a)$, was measured by using the standard dc four-probe technique in parallelepiped form with dimensions $t = 0.5$ mm (thickness), $w = 2$ mm (width), and $l = 10$ mm (length). Before each measurement, the samples were cooled from room temperature down to 77 K.These measurements were done applying an excitation current along the major length of samples, while the magnetic field B_a was applied always perpendicular to the thickness and to the excitation current. Both the voltage across the sample and its temperature were collected while the temperature was raised slowly to 300 K.

3. Results and discussion

Figure 1 shows the powder diffraction patterns of all the samples under study compared to a standard sample. All powders were obtained after grinding in agate mortar to each of the samples. In the diffractograms there are no discernible differences because all the peaks are in the angles seen in the pattern there are only some differences in the intensities of some of them which can be attributed to the fact that fraction of extra phases varies with doping of α-Al_2O_3 NPs as reported by Ghattas *et al*. [3] which will be investigated in detail in future articles using the Rietveld refinement method [16].

Figure 2 shows the dependence of the electrical resistivity as a function of the temperature at zero magnetic field. Note that the critical temperature value of all samples is below 105 K. However, all samples have a critical temperature higher than to that corresponding to the sample B00 which is not doped with α-Al_2O_3 NPs. The sample B03, which has 0.3% by weight of α-Al_2O_3 NPs, has the highest critical temperature value of all of samples. From these results it can be inferred that doping with α-Al_2O_3 NPs favors the increase of the critical temperature value of this type of material. Later on, this physical fact will be examined in order to determine more precisely whether the increase in critical temperature always leads to improvements in the transport properties of these materials.

Figure 3 was obtained from the critical temperature values of each sample determined in Fig. 2 and it can be noticed with more precision what these values are for each one of the samples under study. The highest value corresponds to sample B03 and is $T_c \approx 102$ K.

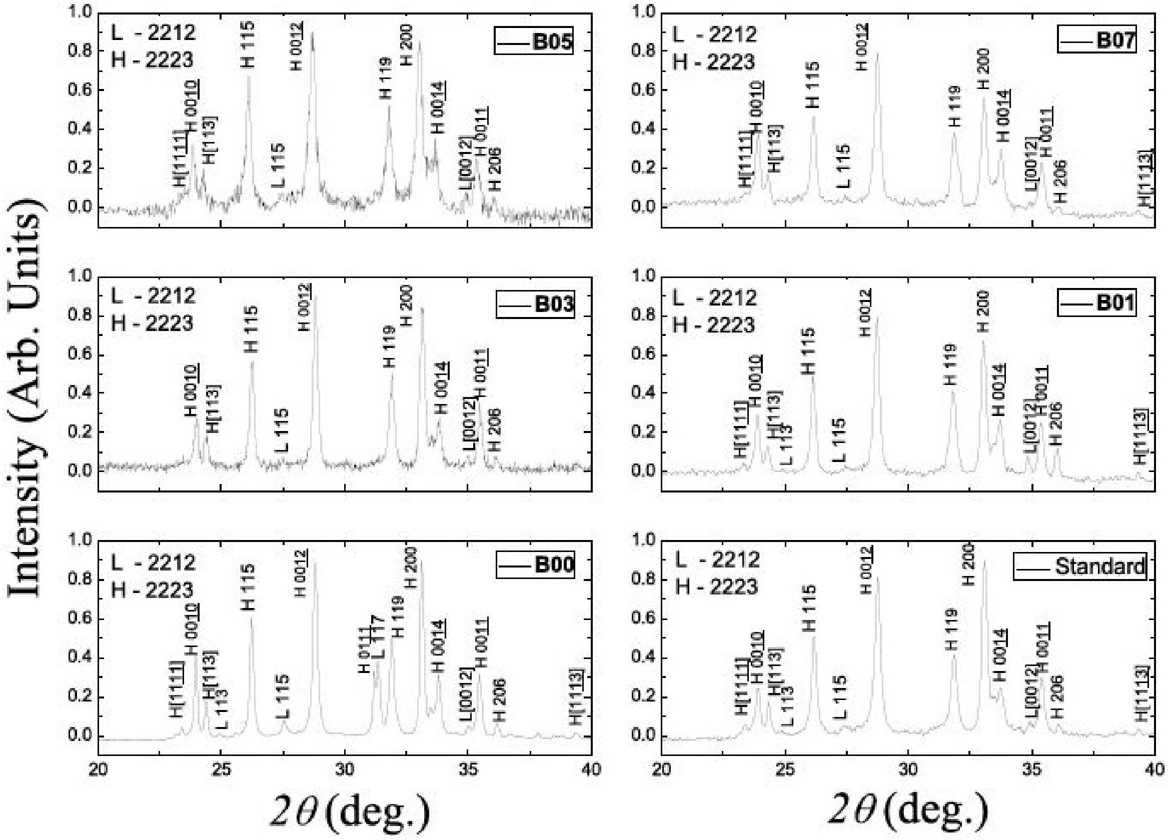

FIGURE 1. X-ray diffraction patterns of the powder samples doped with different % wt. of α-Al_2O_3 NPs.

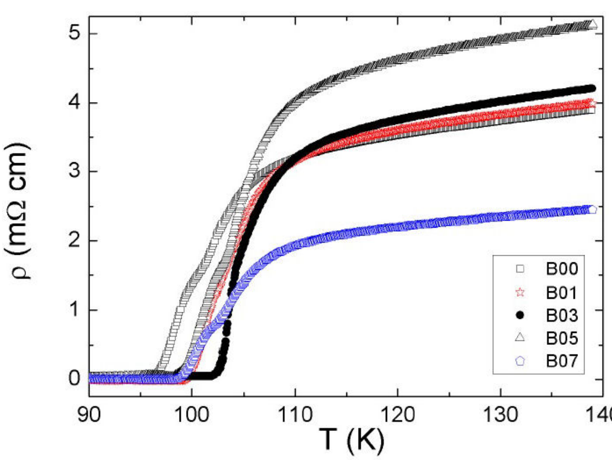

FIGURE 2. Temperature dependence of electrical resistivity, $\rho(T)$, in zero applied magnetic field of the samples doped with different % wt. of α-Al_2O_3 NPs.

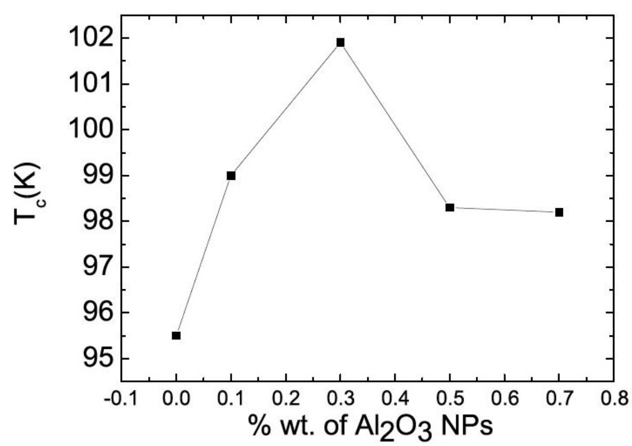

FIGURE 3. Critical temperature dependence of the % wt. of α-Al_2O_3 NPs.

Figure 4 shows the Arrhenius plot corresponding to sample B00. By means of linear fits in the transition region, the values of the effective pinning energy are obtained for each of the magnetic field values shown in the figure. Thus, to obtain Fig. 5, the same procedure used in Fig. 4 was used for the remainder of the samples. This procedure is based on the equation of the Arrhenius plot [17, 18]:

$$\rho(T) = \rho_0 \exp\left\{-\frac{U(B_a,T)}{k_B T}\right\}, \qquad (1)$$

where, for $B_a \leq 10$ mT,

$$U(B_a,T) = U_0(B_a)(1 - T/T_{c0}),$$

far form it

$$U(B_a,T) = U_0(B_a)(T_{c0}/T - 1).$$

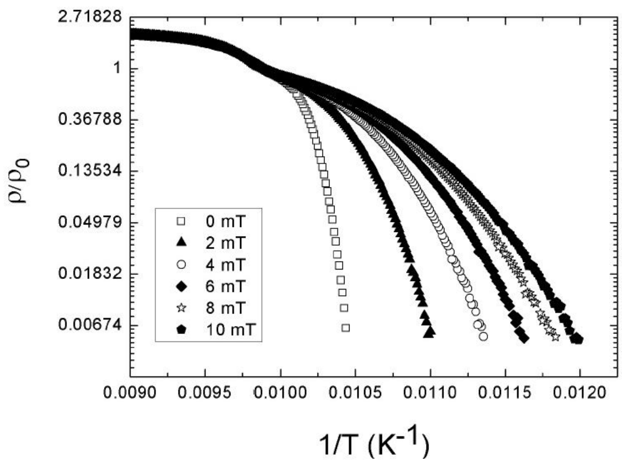

FIGURE 4. Example of the typical Arrhenius plot of the samples under study; This case corresponds to sample B00. By means of fits of these curves in the region of the resistive transition the values of effective pinning energy are obtained as a function of the magnetic field.

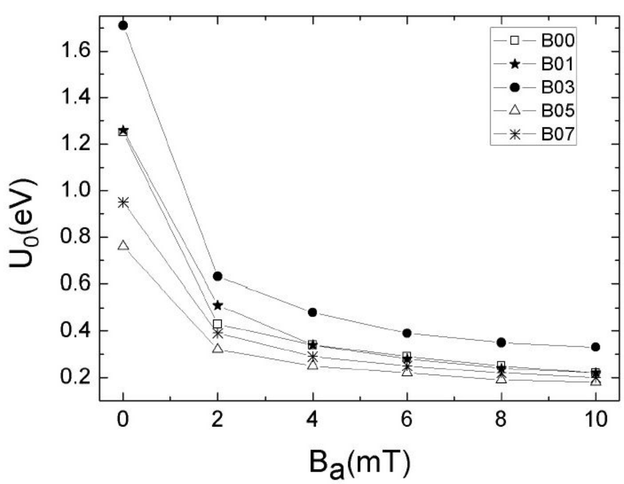

FIGURE 5. Effective pinning energy dependence with the applied magnetic field, Ba, of samples doped with different % wt. of α-Al_2O_3 NPs.

Moreover, k_B is the Boltzmann constant, T_{c0} is the temperature where the curves the temperature at which the curves are separated y ρ_0 is the electrical resistivity when $T = T_{c0}$.

In Fig. 5 it can be seen that the sample B03 has the highest values of effective pinning energy in the region of the magnetic field analyzed. Although not in perfect agreement with the results of Ghattas *et al*. [1, 3], it does not deviate from the results obtained by them. This difference must have its causes in the process of obtaining the samples, which was remarked in the experimental part. In addition to the fact that the route to be followed is not the same (see Table I), there are studies that have studied the effects of compacting pressure on the microstructure and on the properties of electric transport where the most important thing is that with the increase of the compacting pressure increases the texture, the coupling of the weak links and consequently improve their properties of electrical transport [4, 5, 19]. Ghattas *et al*. [3] used 1 GPa which is a high pressure compared to that used in our work. Another issue is the sintering temperature which are also different in both methods but in turn the time of the last sinterization is very different. P. Kameli *et al*. [20] studied the effects of the sintering temperature on the properties of superconductors of the Bi-2223 system and obtained that the increase of the same causes the reduction of the fraction of extra phase Bi-2212 and that causes a better' In the properties of the samples. So there are several factors that make the results obtained in this article are not exactly the same as those obtained by Ghattas *et al.* [3]. However, this result corroborates the findings of Ghattas *et al*. [1, 3] that up to 0.3% by weight of α-Al_2O_3 NPs do not modify the structure of the system (Bi, Pb) -2223. Note that the sample B00 has an intermediate behavior as regards the values of the effective pinning energy, which reaffirms the above: it can be seen that above that curve tend to be those of the samples whose % wt. of α-Al_2O_3 NPs ratio is less than or equal to 0.3% and below which correspond to a weight percent greater than 0.3%. In addition, the values corresponding to the sample B05 are the lowest of the whole set of samples under study. From this it can be argued that sample B03 is the one with the best transport properties and B05 is the one with the worst transport properties.

4. Conclusions

In summary, in this preliminar study of the doping with nanosize α-Al_2O_3 (40 nm) effects in the transport properties of (Bi,Pb)-2223 ceramic samples, it was noted that the sample B03 has the best transport properties in the superconducting state. This fact was observed in the dependence of the effective pinning energy as a function of the magnetic field. Taking into account the techniques used in this preliminary study, we can select some of the samples from this set to study more specific questions about the effect of doping: one that does not contain α-Al_2O_3 NPs (B00), the best transport properties (B03) and the worst transport properties (B05). A further detailed study of samples B00, B03 and B05 could continue to shed light on the understanding of the mechanisms of penetration, trapping and relaxation of the magnetic flux in these materials.

Acknowledgments

This work was supported by the Fundação Coordenação de Aperfeiçoamento de Pessoal de Nível Superior (CAPES) under Grant No. 104/10.

1. A. Ghattas, F. Ben Azzouz, M. Annabi, M. Zouaoui and M. Ben Salem, *Journal of Physics: Conference Series* **97** (2008) 012175.
2. D. Larbalestier, A. Gurevich, D. Matthew Feldmann, and A. Polyanskii, *Nature* **414** (2001) 368.
3. A. Ghattas, M. Annabi, M. Zouaoui, F. Ben Azzouz, and M. Ben Salem, *Physica C* **468** (2008) 31-38.
4. E. Govea-Alcaide, P. Muné and R.F. Jardim, *Physica C* **408-410** (2004) 56-57.
5. E. Govea-Alcaide, P. Muné and R.F. Jardim, *Physica C* **408-410** (2004) 711.
6. N.V. Vo, H.K. Liu and S.X. Dou, *Supercond. Sci. Technol.* **9** (1996) 104-112.
7. R.C. Ma *et al*., *Physica C* **405** (2004) 34.
8. M. Annabi, A. Mchirgui, F. Ben Azzouz, M. Zouaoui and M. Ben Salem, *Physica C* **405** (2004) 34.
9. I.E. Agranovski, A.Y. Ilyushechkin, I.S. Altman, T.E. Bostrom and M. Choi, *Physica C* **434** (2006) 115.
10. A. Amira *et al*., *Physica C* **471** (2011) 1621-1626.
11. P. Muné, M. Hernández-Wolpez, A. Cruz-García and R.F. Jardim, *Rev. Cub. Fís.* **32** (2015) 53-55
12. M. Hernández-Wolpez, A. Cruz-García , O. Vázquez-Robaina, R.F. Jardim and P. Muné, *Physica C* **525-526** (2016) 84-88.
13. M. Hernández-Wolpez, A. Cruz-García, R.F. Jardim and P. Muné, *J. Mater. Sci: Mater. Electron.* **28** (2017) 15246-15251.
14. V.E. Gasumyants *et al Sov. Supercond.* **4** (1991) 504.
15. P. Muné, E. Govea-Alcaide and R.F. Jardim, *Physica C* **384** (2003) 491.
16. H.M. Rietveld, *J. Appl. Cryst.* **2** (1969) 65.
17. A.J. Batista-Leyva, R. Cobas, M.T.D. Orlando and E. Altshuler, *Supercond. Sci. Technol.* **16** (2003) 857.
18. E. Govea-Alcaide, M. Hernández-Wolpez, A.J. Batista-Leyva, R.F. Jardim and P. Muné, *Physica C* **423** (2005) 51.
19. E. Govea-Alcaide, R.F. Jardim and P. Muné, *Physica C* **423** (2005) 152.
20. P. Kameli, H. Salamati and M. Eslami, *Solid State Communications* **137** (2006) 30.